

Geometric Requirements for Tectorial Membrane Traveling Waves in the Presence of Cochlear Loads

Jonathan B. Sellon,^{1,2,*} Roozbeh Ghaffari,² and Dennis M. Freeman^{1,2,3}

¹Harvard–MIT Program in Health Sciences and Technology, ²Research Laboratory of Electronics, and ³Department of Electrical Engineering and Computer Science, Massachusetts Institute of Technology, Cambridge, Massachusetts

ABSTRACT Recent studies suggest that wave motions of the tectorial membrane (TM) play a critical role in determining the frequency selectivity of hearing. However, frequency tuning is also thought to be limited by viscous loss in subtectorial fluid. Here, we analyze effects of this loss and other cochlear loads on TM traveling waves. Using a viscoelastic model, we demonstrate that hair bundle stiffness has little effect on TM traveling waves calculated with physiological parameters, that the limbal attachment can cause small (<20%) increases in TM wavelength, and that viscous loss in the subtectorial fluid can cause small (<20%) decreases in TM wave decay constants. However, effects of viscous loss in the subtectorial fluid are significantly increased if TM thickness is decreased. In contrast, increasing TM thickness above its physiological range has little effect on the wave, suggesting that the TM is just thick enough to maximize the spatial extent of the TM traveling wave.

The mammalian inner ear separates low-intensity sounds by their frequency content, and loss of this frequency selectivity impairs our ability to understand speech, especially in noisy environments. These extraordinary properties of hearing depend on traveling waves of motion that propagate along both the basilar membrane and tectorial membrane (TM), ultimately stimulating mechanosensory receptors. Classical models of cochlear mechanics suggest that the spectral resolution of hearing is limited by viscous damping in the subtectorial fluid, and that cochlear amplification is required to compensate (1–6). However, several studies have shown that wave motions of the TM may play an important role in determining frequency tuning in a fundamentally different way—by longitudinally coupling many sensory receptor cells (7–12). In these studies, frequency tuning is determined by the wave properties (speed and decay constant) of TM traveling waves. These wave properties depend on material properties of the TM (shear storage modulus, G' , and shear viscosity, η) (7,13,14), as well as cochlear loads, including viscous damping in the subtectorial fluid. Here we analyze the effects of cochlear loads on a TM traveling wave model, and show that they have little effect on TM waves, provided that the TM is thick enough to support the wave despite dissipation from the subtectorial fluid.

Shearing motions of an isolated TM can be represented by a series of masses (m) that are viscoelastically coupled by the parallel combination of springs (k) and dashpots (b) (Fig. 1, A and B). These parameters can be related to the following material properties and geometrical factors: $m = \rho WT\Delta$, $k = G'(WT/\Delta)$, and $b = \eta(WT/\Delta)$, where W is the width of the TM; T is the thickness of the TM in the transverse dimension; Δ is the length of each longitudinal section; and ρ is the density of the TM, taken to be that of water.

Alternatively, shearing motions of an isolated TM can be represented by the following differential equation:

$$F = ma = WT\Delta\rho\ddot{x} = WT\Delta G' \frac{\partial^2 x}{\partial z^2} + WT\Delta\eta \frac{\partial^2 \dot{x}}{\partial z^2}, \quad (1)$$

where x is the radial displacement of the TM.

To determine the distance over which viscoelastic coupling is significant, we generate a radial displacement x on the TM and determine the wave decay constant σ , which is the longitudinal distance over which the amplitude of the wave decays by a factor of e . Assuming $x = \Re\{X e^{j(\omega t - k_n z)}\}$, we can solve for the wave number k_n :

$$k_n^2 = \frac{\rho\omega^2}{G' + j\omega\eta}. \quad (2)$$

From k_n , we can calculate the wavelength $\lambda = (2\pi/\Re\{k_n\})$ and the wave decay constant $\sigma = -(1/\Im\{k_n\})$.

Submitted December 21, 2016, and accepted for publication February 3, 2017.

*Correspondence: sellon@mit.edu

Editor: Jeffrey Fredberg.

<http://dx.doi.org/10.1016/j.bpj.2017.02.002>

© 2017 Biophysical Society.

This is an open access article under the CC BY-NC-ND license (<http://creativecommons.org/licenses/by-nc-nd/4.0/>).



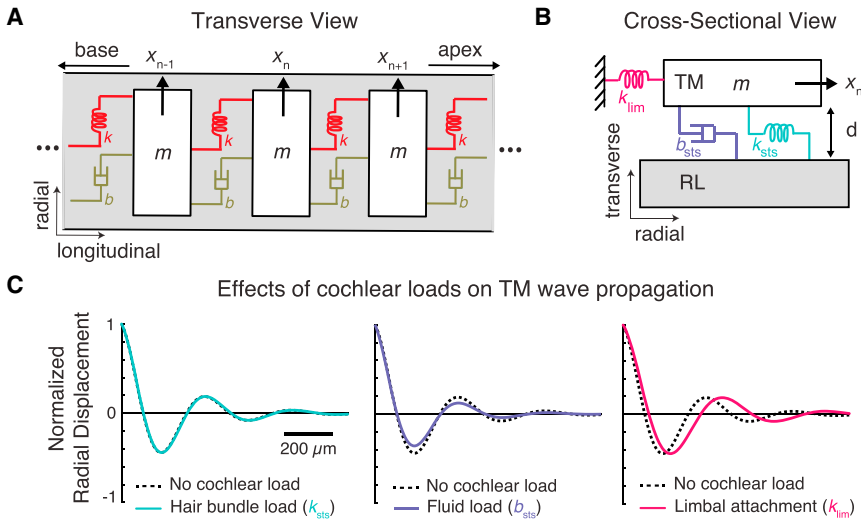


FIGURE 1 Effects of cochlear loads on TM traveling waves. **(A)** TM section consisting of a mass (m) coupled to adjacent sections by viscous (b) and elastic (k) components. Radial displacements of the TM (x_n) are generated by stimulating a single radial cross section of the TM (at $n = 0$), which is then coupled to neighboring regions. **(B)** Cross-sectional view of a TM section and underlying cochlear loads (hair bundle stiffness k_b , limbal attachment k_{lim} , and subtektorial fluid load b_{sts}). **(C)** Radial TM displacement as a function of longitudinal distance (l). Adding hair bundle stiffness ($k_b = 0.0035$ N/m) to the model increased space constants by $\sim 1\%$. Adding a limbal attachment (k_{lim} , assuming $T_l = 10 \mu\text{m}$ and $W_l = 100 \mu\text{m}$) had little effect on reducing TM spatial extent, but increases wavelengths by $\sim 19\%$. Viscous damping in the subtektorial space (b_{sts} , assuming a $2 \mu\text{m}$ fluid gap) decreased σ by $\sim 20\%$ to $180 \mu\text{m}$.

Results for 20 kHz stimulation (Fig. 1 C) with $G' = 47$ kPa, $\eta = 0.22$ Pa \cdot s, $W = 100 \mu\text{m}$, $T = 30 \mu\text{m}$ (chosen based on previous measurements of basal TM regions (7,11,15)), and an initial radial displacement of $x = 1$ nm (chosen based on previous measurements of basilar membrane vibration magnitudes at threshold (16)), are illustrated with dashed waveforms in Fig. 1 C, where the resulting wave decay constant $\sigma = 223.7 \mu\text{m}$. To study the effects of cochlear hair bundles on TM traveling waves, we added an expression to represent the force ($-nk_b\Delta(x/s)$) due to hair bundle stiffness to Eq. 1, where k_b is the stiffness of a single outer hair cell bundle, $n = 2$ is the number of rows of outer hair cells, and $s \sim 10^{-5}$ m is the longitudinal distance between adjacent hair cells. Including the load from hair bundles ($k_b = 3.5$ mN/m (17)) resulted in an $\sim 1\%$ change in TM wave decay constant (Fig. 1 C, left panel). To test the generality of this result, we increased k_b by up to $10\times$ and observed similarly small effects on TM spatial extent (Fig. S1 in the Supporting Material). To study the effects of the limbal attachment on TM traveling waves, we added an expression to represent the force ($-3G'\Delta T_l(x/W_l)$) due to the limbal attachment to Eq. 1, where T_l is the height and W_l is the width of the limbal attachment. Including the load from the limbal attachment also had little effect on spatial extent of the TM wave, but increased wavelengths by $\sim 19\%$ (Fig. 1 C, right panel).

At very low frequencies, the fluid velocity profile in the subtektorial gap is linear, and the fluid load ($-W\Delta\mu(\dot{x}/d)$) can be added to Eq. 1, where d represents the thickness of the subtektorial gap and μ is the viscosity of the subtektorial fluid, taken to be the viscosity of water. Including just the load from fluid viscosity in the subtektorial gap (Couette flow with a subtektorial space height (d) of $2 \mu\text{m}$ (18)) reduced TM wave decay constants by $\sim 20\%$ to $\sim 179.6 \mu\text{m}$ (Fig. 1 C, middle panel). More generally, the fluid load

depends on frequency and affects both the bottom and top surfaces of the TM. Wave decay constants for this more general model are within $\sim 12\%$ of those predicted by the Couette model (Fig. S2).

These results suggest that while neither hair bundle stiffness nor the limbal attachment have a significant effect on the spatial extent of TM waves, fluid loads in the subtektorial space do. To understand how the TM can support waves despite these external fluid loads, we examined the magnitude of the TM waves for a variety of TM thicknesses (Fig. 2 A, left panel) and subtektorial gap heights (Fig. 2 A, right panel). Assuming hair bundle and subtektorial fluid loads,

$$k_n^2 = \frac{WT\rho\omega^2 - 3\frac{k_b}{s} - W\mu\frac{j\omega}{d}}{WT(G' + j\omega\eta)}, \quad (3)$$

and the resulting TM wave decay constant is $180.8 \mu\text{m}$. As the TM's thickness is reduced to one-third of its physiologic value (thus reducing its mass (m), stiffness (k), and damping (b)) the wavelength remains relatively unchanged, but the spatial extent of the wave is significantly reduced by 28% to $\sigma = 129.5 \mu\text{m}$. In contrast, increasing the TM's thickness to three times its physiological value increases the space constant by 14% to $\sigma = 207.5 \mu\text{m}$. Thus, the wave nature of the motion for natural TM thicknesses ($T = 30 \mu\text{m}$) is slightly more prominent when the TM thickness is increased by a factor of 3, and almost completely damped when the TM thickness is reduced by a factor of 3 (Fig. 2 A, left panel). Similarly, as the subtektorial gap is reduced the spatial extent of the wave is reduced due to increased external fluid load (Fig. 2 A, right panel).

The effect of the subtektorial space on wave properties is thus small when the TM is thick ($>90 \mu\text{m}$) and large when the TM is thin ($<10 \mu\text{m}$). To determine the critical thickness

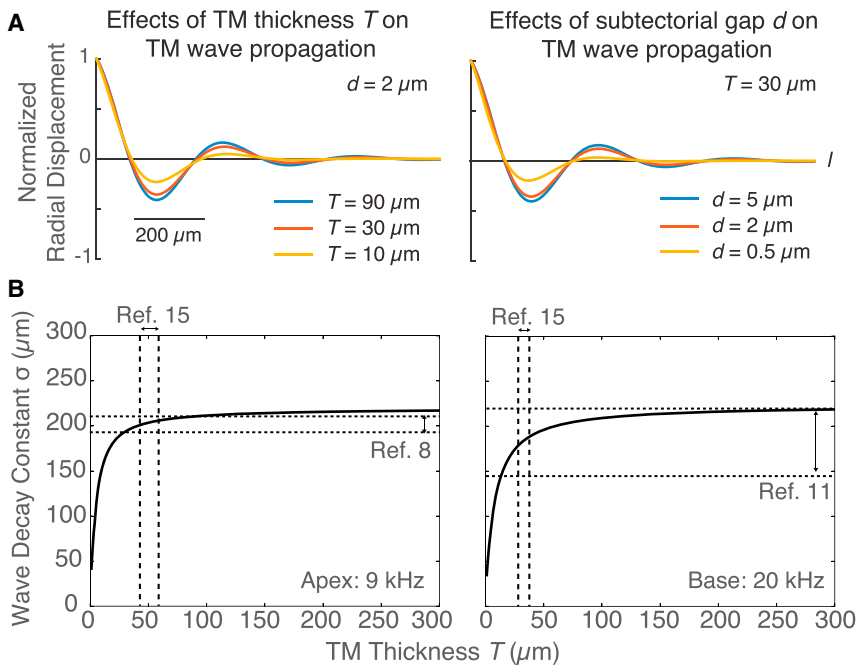


FIGURE 2 Effects of TM thickness and subtektorial gap on TM traveling waves as a function of longitudinal distance (l). (A) TM wave propagation in the presence of cochlear loads for three TM thicknesses (left panel, $T = 10, 30,$ and $90 \mu\text{m}$, assuming $d = 2 \mu\text{m}$) and subtektorial gaps (right panel, $d = 0.5, 2,$ and $5 \mu\text{m}$, assuming $T = 30 \mu\text{m}$), given $G' = 47 \text{ kPa}$, $\eta = 0.22 \text{ Pa}\cdot\text{s}$, and $W = 100 \mu\text{m}$. (B) TM wave decay constant as a function of TM thickness for both apical (right panel; $W = 175 \mu\text{m}$, $d = 5 \mu\text{m}$, $G' = 18 \text{ kPa}$, and $\eta = 0.21 \text{ Pa}\cdot\text{s}$) and basal (left panel; $W = 100 \mu\text{m}$, $d = 2 \mu\text{m}$, $G' = 47 \text{ kPa}$, and $\eta = 0.22 \text{ Pa}\cdot\text{s}$) TM regions. The predicted wave decay constants fall within the range of previously measured TM wave decay constants (thin dashed lines, interquartile range at 20 kHz (11) and range from 9 to 11 kHz (8)) based on previous measurements of TM thickness (thick dashed lines (15)). These values were chosen to match physiologic measurements for the subtektorial gap (18) and mouse TM material properties (7,8,11).

at which the loads begin to affect the TM traveling wave, we calculated wave decay constants as a function of thickness (Fig. 2 B). Given apical (Fig. 2 B, right panel) and basal (Fig. 2 B, left panel) TM material properties, a plateau exists where further increasing TM thickness has little effect on the spatial extent of TM waves. For basal TM regions at physiological thickness, the TM wave decay constants are $\sim 17\%$ below this maximum possible spatial decay constant. Thus, we see that increasing TM thickness beyond its physiological thickness (26–33 μm in the cochlear base, 43–59 μm in the cochlear apex (15)) has little effect on the TM traveling wave. The spatial extents predicted given these TM dimensions also match well with physiologic measurements of the spatial extent of basal TM waves at 20 kHz and apical TM waves at 9 kHz (8,11) (Fig. 2 B, thin dashed lines). We also examined spatial extent of TM waves for fluid load based on the Couette model versus a boundary layer fluid (Fig. S3), and see a similar dependence on TM thickness.

Altering the thickness of the TM changes three parameters in the model (G' , η , and ρ). To determine which of these is most responsible for the trends shown in Fig. 2 B, we vary each material property separately while holding the others at their nominal values. Results in Fig. S4 demonstrate that the overall dependence of wave decay constant on thickness is not dominated by any single material property.

In addition to predicting the spatial extent of wild-type TMs, we calculated those of mutant TMs, such as those lacking β -tectorin (19). Fig. S5 demonstrates that the predicted wave decay constants lie well within previously measured spatial extents of $Tectb^{-/-}$ TM waves given $Tectb^{-/-}$ TM material properties and thicknesses (8).

Our results demonstrate that a minimum TM thickness is required to support traveling waves. Viscous damping in the subtektorial space has little effect on TM traveling waves if the TM is thick, but large effect if the TM is thin. The TM's natural thickness is just large enough so that TM traveling waves persist with little effect of viscous damping in the subtektorial space. Furthermore, the thicker TM of the cochlear apex (15) is necessary to support the larger TM wave decay constants associated with low-frequency cochlear regions (8), thus providing a physical basis for systematic changes in TM thickness throughout the cochlea. Combined, these results suggest that there could have been evolutionary pressure to drive the TM to be just thick enough to support a traveling wave despite damping from the subtektorial fluid space.

SUPPORTING MATERIAL

Five figures are available at [http://www.biophysj.org/biophysj/supplemental/S0006-3495\(17\)30157-1](http://www.biophysj.org/biophysj/supplemental/S0006-3495(17)30157-1).

AUTHOR CONTRIBUTIONS

J.B.S., R.G., and D.M.F. designed the research; J.B.S. and D.M.F. analyzed the model; and J.B.S., R.G., and D.M.F. wrote the article.

ACKNOWLEDGMENTS

We thank John J. Guinan Jr. and Christopher A. Shera for their helpful comments and suggestions on this work.

This work was supported by National Institutes of Health (NIH) grant No. R01-DC00238, and J.B.S. was supported by the National Science

Foundation Graduate Research Fellowship Program (NSF GRFP) under grant No. 1122374.

REFERENCES

1. Allen, J. B. 1980. Cochlear micromechanics—a physical model of transduction. *J. Acoust. Soc. Am.* 68:1660–1670.
2. Mammano, F., and R. Nobili. 1993. Biophysics of the cochlea: linear approximation. *J. Acoust. Soc. Am.* 93:3320–3332.
3. Zwislocki, J. J. 1980. Five decades of research on cochlear mechanics. *J. Acoust. Soc. Am.* 67:1679–1685.
4. Guinan, J. J., Jr. 2012. How are inner hair cells stimulated? Evidence for multiple mechanical drives. *Hear. Res.* 292:35–50.
5. Prodanovic, S., S. Gracewski, and J. H. Nam. 2015. Power dissipation in the subtectorial space of the mammalian cochlea is modulated by inner hair cell stereocilia. *Biophys. J.* 108:479–488.
6. Wang, Y., and E. S. Olson. 2016. Cochlear perfusion with a viscous fluid. *Hear. Res.* 337:1–11.
7. Ghaffari, R., A. J. Aranyosi, and D. M. Freeman. 2007. Longitudinally propagating traveling waves of the mammalian tectorial membrane. *Proc. Natl. Acad. Sci. USA.* 104:16510–16515.
8. Ghaffari, R., A. J. Aranyosi, ..., D. M. Freeman. 2010. Tectorial membrane travelling waves underlie abnormal hearing in *Tectb* mutant mice. *Nat. Commun.* 1:96.
9. Meaud, J., and K. Grosh. 2010. The effect of tectorial membrane and basilar membrane longitudinal coupling in cochlear mechanics. *J. Acoust. Soc. Am.* 127:1411–1421.
10. Lee, H. Y., P. D. Raphael, ..., J. S. Oghalai. 2015. Noninvasive in vivo imaging reveals differences between tectorial membrane and basilar membrane traveling waves in the mouse cochlea. *Proc. Natl. Acad. Sci. USA.* 112:3128–3133.
11. Sellon, J. B., R. Ghaffari, ..., D. M. Freeman. 2014. Porosity controls spread of excitation in tectorial membrane traveling waves. *Biophys. J.* 106:1406–1413.
12. Sellon, J. B., S. Farrahi, ..., D. M. Freeman. 2015. Longitudinal spread of mechanical excitation through tectorial membrane traveling waves. *Proc. Natl. Acad. Sci. USA.* 112:12968–12973.
13. Jones, G. P., V. A. Lukashkina, ..., A. N. Lukashkin. 2013. Frequency-dependent properties of the tectorial membrane facilitate energy transmission and amplification in the cochlea. *Biophys. J.* 104:1357–1366.
14. Gavara, N., and R. S. Chadwick. 2010. Noncontact microrheology at acoustic frequencies using frequency-modulated atomic force microscopy. *Nat. Methods.* 7:650–654.
15. Keiler, S., and C. P. Richter. 2001. Cochlear dimensions obtained in hemicochleae of four different strains of mice: CBA/CAJ, 129/CD1, 129/SvEv and C57BL/6J. *Hear. Res.* 162:91–104.
16. Robles, L., and M. A. Ruggero. 2001. Mechanics of the mammalian cochlea. *Physiol. Rev.* 81:1305–1352.
17. Kennedy, H. J., A. C. Crawford, and R. Fettiplace. 2005. Force generation by mammalian hair bundles supports a role in cochlear amplification. *Nature.* 433:880–883.
18. Furness, D. N., S. Mahendrasingam, ..., C. M. Hackney. 2008. The dimensions and composition of stereociliary rootlets in mammalian cochlear hair cells: comparison between high- and low-frequency cells and evidence for a connection to the lateral membrane. *J. Neurosci.* 28:6342–6353.
19. Russell, I. J., P. K. Legan, ..., G. P. Richardson. 2007. Sharpened cochlear tuning in a mouse with a genetically modified tectorial membrane. *Nat. Neurosci.* 10:215–223.